

---

# Diffusion-Weighted Magnetic Resonance Imaging for the Diagnosis of Lymph Node Metastasis in Patients with Biliary Tract Cancer

---

[Takashi Murakami](#) , [Hiroaki Shimizu](#) \* , [Hiroyuki Nojima](#) , Kiyohiko Shuto , [Akihiro Usui](#) , [Chihiro Kosugi](#) , Keiji Koda

Posted Date: 25 August 2024

doi: 10.20944/preprints202408.1694.v1

Keywords: Diffusion-weighted imaging; magnetic resonance imaging; lymph node metastasis; biliary tract cancer; diagnostic accuracy



Preprints.org is a free multidiscipline platform providing preprint service that is dedicated to making early versions of research outputs permanently available and citable. Preprints posted at Preprints.org appear in Web of Science, Crossref, Google Scholar, Scilit, Europe PMC.

Copyright: This is an open access article distributed under the Creative Commons Attribution License which permits unrestricted use, distribution, and reproduction in any medium, provided the original work is properly cited.

Disclaimer/Publisher's Note: The statements, opinions, and data contained in all publications are solely those of the individual author(s) and contributor(s) and not of MDPI and/or the editor(s). MDPI and/or the editor(s) disclaim responsibility for any injury to people or property resulting from any ideas, methods, instructions, or products referred to in the content.

Article

# Diffusion-Weighted Magnetic Resonance Imaging for the Diagnosis of Lymph Node Metastasis in Patients with Biliary Tract Cancer

Takashi Murakami, Hiroaki Shimizu \*, Hiroyuki Nojima, Kiyohiko Shuto, Akihiro Usui, Chihiro Kosugi and Keiji Koda

Department of Surgery, Teikyo University Chiba Medical Center, Ichihara, Japan

\* Correspondence: h-shimizu@med.teikyo-u.ac.jp

**Abstract: Objective:** The diagnostic efficacy of the apparent diffusion coefficient (ADC) on diffusion-weighted magnetic resonance imaging for lymph node metastasis in biliary tract cancer was investigated in the present study. **Methods:** Surgically resected 112 lymph nodes from 35 biliary tract cancer patients were examined in this study. Values of the ADC mean and minimum of lymph nodes, as well as short-axis and long-axis diameters of lymph nodes were assessed by computed tomography (CT). The relationship between these parameters and the presence of histological lymph node metastasis was evaluated. **Results:** Histological lymph node metastasis was detected in 31 (27.7%) out of 112 lymph nodes. The short-axis diameter in metastatic lymph nodes was significantly larger than that in non-metastatic lymph nodes ( $P = 0.002$ ), but the long-axis diameter was not significantly different between metastatic and non-metastatic lymph nodes. Both ADC mean and minimum values in metastatic lymph nodes were significantly lower than those in non-metastatic lymph nodes ( $P < 0.001$ , respectively). However, the ADC minimum value showed the highest accuracy for the diagnosis of histological lymph node metastasis, with an area under the curve of 0.877, sensitivity of 87.1%, specificity of 82.7%, and accuracy of 83.9%. **Conclusions:** The ADC minimum value on diffusion-weighted magnetic resonance imaging was very useful for the diagnosis of lymph node metastasis in biliary tract cancer.

**Keywords:** Diffusion-weighted imaging; magnetic resonance imaging; lymph node metastasis; biliary tract cancer; diagnostic accuracy

---

## Introduction

Biliary tract cancer includes intrahepatic cholangiocarcinoma, perihilar cholangiocarcinoma, distal cholangiocarcinoma, gallbladder cancer, and ampullary cancer. Biliary tract cancer is a rare malignancy, with an incidence of approximately 6 per 100,000 people, but the overall incidence of biliary tract cancer is increasing due to the increase in intrahepatic cholangiocarcinoma [1]. Contrast-enhanced dynamic computed tomography (CT) and magnetic resonance imaging (MRI) are effective for assessing the primary lesion, the extent of disease, and vascular invasion. Endoscopic retrograde cholangiopancreatography (ERCP) is useful not only for diagnosing the horizontal extent of cholangiocarcinoma but also for vertical extent diagnosis with intraductal ultrasonography, as well as for pathological diagnosis through cytology or bile duct biopsy. ERCP also allows for biliary drainage for obstructive jaundice. Endoscopic ultrasonography has high diagnostic capability for qualitative diagnosis and vascular invasion. Positron emission tomography (PET) is useful for detecting metastases and diagnosing postoperative recurrence.

Surgical resection is the only curative treatment for biliary tract cancer, however, various factors can lead to unresectability. Surgical treatment is highly invasive and often involves concomitant liver resection, so the patient's overall condition and factors such as decreased liver function may result in a determination of unresectability [2]. Biliary tract cancer with distant metastasis is generally considered unresectable. However, there are cases where finally treated by conversion surgery after long-term chemotherapy [3].

The prognosis of biliary tract cancer remains poor among gastrointestinal cancers, with a 5-year survival rate of 24-61% [4]. Lymph node metastasis has been shown to be an independent prognostic factor in biliary tract cancer, including extrahepatic bile duct cancer, gallbladder cancer, and ampullary cancer [5-7]. Furthermore, in cases of distal cholangiocarcinoma, a good prognosis can be expected with curative resection when the number of metastatic lymph nodes is two or fewer [8]. In gallbladder cancer, the number of metastatic lymph nodes is considered a poor prognostic factor [6]. For ampullary cancer, cases with four or more metastatic lymph nodes have been reported to have a poorer prognosis compared to cases with three or fewer [9]. Matsuyama et al. demonstrated that lymph node metastasis and vascular invasion are poor prognostic factors in perihilar cholangiocarcinoma [10]. In a subsequent report, they administered neoadjuvant chemotherapy with a combination of gemcitabine and S-1, a combined drug of tegafur, gimestat and otastat potassium, to perihilar cholangiocarcinoma patients with risks including lymph node metastasis and reported favorable outcomes, with a disease control rate of 91.3%, a median survival time of 30.3 months, and a 5-year survival rate of 30%. Additionally, the resection rate in the cohort was 71%, and among the resected cases, the R0 resection rate was 81% [11]. Therefore, accurate diagnosis of preoperative lymph node metastasis is essential for biliary tract cancer.

Preoperative diagnosis of lymph node metastasis is usually performed by CT, MRI, and PET [12]. Previous reports revealed that the long-axis diameter in metastatic lymph nodes was larger than that of non-metastatic lymph nodes, and the long-axis diameter correlated with the area of cancer within lymph nodes [13]. However, diagnosis using the long-axis diameter of lymph nodes was considered to have low accuracy for identifying metastatic lymph nodes. Therefore, in various types of cancer, the short-axis diameter of lymph nodes has been previously used for diagnosing lymph node metastasis [14,15]. However, when evaluating only the short-axis diameter of lymph nodes, lymph node swelling due to inflammation may be misdiagnosed as lymph node metastasis. Noji et al. concluded that CT diagnosis is no longer useful for determining lymph node metastasis in biliary tract cancer [16].

Proliferated tumor cells increase cellular density and suppress the diffusion of water molecules, leading to higher signal intensity in diffusion-weighted MRI (DW-MRI) [17]. The apparent diffusion coefficient (ADC) value quantitatively represents this magnitude of diffusion, which can be applied to differentiate malignant tumors from normal tissues [17]. The ADC value in pancreatic cancer has been reported to be associated with the degree of tumor differentiation and selected as an independent prognostic factor [18]. This result indicates that the ADC value reflects tumor malignancy. Moreover, DW-MRI has been reported to be useful for distinguishing between malignant and benign biliary tract diseases. In differentiating gallbladder cancer from cholecystitis, the ADC value in gallbladder cancer was significantly lower than in cholecystitis [19,20]. Similarly, DW-MRI was effective for differentiating bile duct cancer from benign biliary stricture [21]. More recently, Miyazaki et al. reported that the low ADC minimum value in the primary lesion of intrahepatic cholangiocarcinoma was significantly correlated with low tumor-infiltrating lymphocytes and was shown to be an independent poor prognostic factor, suggesting the usefulness of the ADC minimum value [22]. In the present study, we investigated the diagnostic performance of DW-MRI for lymph node metastasis in biliary tract cancer.

## Materials and Methods

### *Patients*

Biliary tract cancer patients who underwent surgical resection at our hospital between April 2017 and April 2021 were included in this study. These patients underwent preoperative abdominal contrast-enhanced dynamic CT (arterial phase, portal phase, equilibrium phase) and MRI examinations. The surgically resected specimens were fixed in 10% formalin, embedded in paraffin, and then pathologically evaluated using hematoxylin and eosin staining. The dissected lymph nodes were examined pathologically for metastasis. The study was conducted in accordance with the

Declaration of Helsinki and was approved by the institutional review board of Teikyo University Chiba Medical Center.

#### *Diagnosis of Lymph Node Metastasis*

Regional and para-aortic lymph nodes detected by both CT and MRI and surgically removed by lymph node dissection were selected as subjects for the present study. The short-axis and long-axis diameters of these lymph nodes were measured by CT (Figure 1a). MRI was performed with a 1.5 T body scanner equipped with a phased array body coil (Signa HDxt 1.5 T; GE Healthcare, Illinois, USA). A single-shot spin-echo type of echo-planar sequence was used to obtain DW-MRI. The fat signals were suppressed using short-tau inversion recovery. The b values corresponding to diffusion-sensitizing gradients were 0 and 1000 s/mm<sup>2</sup>. Sequential sampling of the k-space was used with an effective echo time (TE) and an acquisition matrix of 92 × 192, which was interpolated to 256 × 256 during image calculation. Repetition time (TR) and TE were 12857 ms and 73 ms, respectively. Slices including the upper abdomen were acquired with a 400-mm field of view, a 5-mm slice thickness, and a 1-mm slice gap. T2-weighted images were obtained with the following parameters: TR/TE 618/89, 384 × 224 matrix, 400-mm field of view, and 5-mm section thickness. The ADC mean and minimum values of each lymph node were measured. For quantitative analysis, each annotated lymph node was identified on the corresponding DWI; a region of interest (ROI) for each lymph node was drawn on the ADC map. Circular or oval ROIs were applied to include almost all of the visible lymph nodes; the mean of the ROIs was defined as the ADC mean value and the minimum of the ROIs as the ADC minimum value (Figure 1b-d).

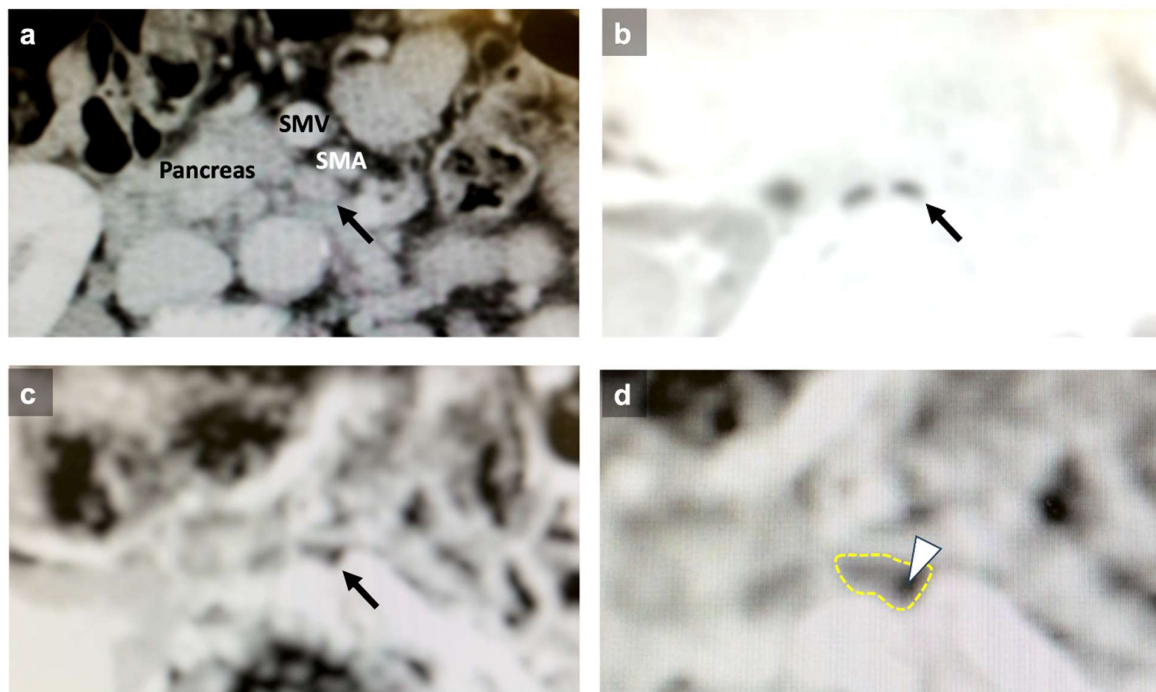


**Figure 1.** CT and MRI findings for the diagnosis of lymph node metastasis. (a) Abdominal CT revealed an enlarged lymph node with a 6.7mm short-axis diameter (arrow). (b) In the DW-MRI, the lymph node showed restricted diffusion (arrow). (c) On the ADC map, the lymph node appeared gray to black (arrow). (d) Magnified image of Figure 1c. The ADC mean value was calculated as the average of the ROI indicated by the yellow dotted line, and the ADC minimum value reflected the area with the lowest ADC value, as shown by the arrowhead. The ADC mean and minimum values were  $1.08 \times 10^{-3} \text{ mm}^2/\text{s}$  and  $0.99 \times 10^{-3} \text{ mm}^2/\text{s}$ , respectively. This lymph node was proven to be metastatic by histological examination. SMA, superior mesenteric artery; SMV, superior mesenteric vein.

### Statistical Analysis

The association between these parameters and histological lymph node metastasis was statistically evaluated by using SPSS Statistics version 21.0 (IBM, New York City, NY, USA). Continuous variables are presented as means and standard deviations". The Mann-Whitney U test was used for continuous variables. The receiver operating characteristic curve was used to assess the diagnostic performance, and cutoff values were determined by Receiver operating characteristic (ROC) curves. The area under the curve, sensitivity, specificity, and accuracy were calculated. A *P* value less than 0.05 was considered statistically significant.

### Results

A total of 35 biliary tract cancer patients were eligible for this study, with 21 males and 14 females (Table 1). The mean age was 73.3 years. The biliary tract cancers in this study included perihilar cholangiocarcinoma (n = 10), intrahepatic cholangiocarcinoma (n = 1), distal cholangiocarcinoma (n = 10), gallbladder carcinoma (n = 10), and ampullary carcinoma (n = 4). The breakdown of surgical procedures included right hemihepatectomy and caudate lobectomy with extrahepatic bile duct resection in 6 cases, left hemihepatectomy and caudate lobectomy with extrahepatic bile duct resection in 6 cases, hepatectomy of segment 4a+5 with extrahepatic bile duct resection in 8 cases, hepatic segmentectomy with extrahepatic bile duct resection in 1 case, and pancreaticoduodenectomy in 14 cases. Eleven (31.4%) patients experienced preoperative cholangitis.

**Table 1.** Patient characteristics (n=35).

| <b>Factors</b>                                  |        |
|---|--------|
| Age, years (mean ± SD)                          | 73 ± 8 |
| Sex   |        |
| Male  | 21     |
| Female  | 14     |
| Anatomical tumor location                       |        |
| Intrahepatic cholangiocarcinoma                 | 1      |
| Perihilar cholangiocarcinoma                    | 10     |
| Distal bile duct cancer                         | 10     |
| Gallbladder cancer                              | 10     |
| Ampullary carcinoma                             | 4      |
| Operative procedure                             |        |
| Right hemihepatectomy + caudate lobectomy + BDR | 6      |
| Left hemihepatectomy + caudate lobectomy + BDR  | 6      |
| Hepatectomy of segment 4a+5 + BDR               | 8      |
| Hepatic segmentectomy + BDR                     | 1      |
| Pancreatoduodenectomy                           | 14     |
| Preoperative cholangitis                        |        |
| Yes   | 11     |
| No  | 24     |
| Lymph nodes to be analyzed                      | 112    |
| pN+   | 31     |
| pN-   | 81     |

SD, standard deviation; BDR, bile duct resection; pN+; pathologically positive lymph node metastasis, pN-; pathologically negative lymph node metastasis.

Thirty-one out of 112 (27.7%) lymph nodes were positive for histological metastases. The distribution of lymph nodes was as follows: common hepatic artery (n = 23), hepatoduodenal ligament (n = 58), around the pancreatic head (n = 20), jejunal mesentery (n = 4), para-aorta (n = 6), and diaphragm (n = 1) (Table 2).

**Table 2.** Details of lymph node locations.

| Locations of lymph nodes | pN+ | pN- | Total |
|--------------------------|-----|-----|-------|
| Common hepatic artery    | 4   | 19  | 23    |
| Hepatoduodenal ligament  | 9   | 49  | 58    |
| Pancreatic head          | 12  | 8   | 20    |
| Jejunal mesentery        | 2   | 2   | 4     |
| Para-aorta               | 3   | 3   | 6     |
| Diaphragm                | 1   | 0   | 1     |
| Total                    | 31  | 81  | 112   |

The short-axis diameter of metastatic lymph nodes ( $6.7 \pm 2.7$  mm) was significantly larger than that of non-metastatic lymph nodes ( $5.1 \pm 2.1$  mm,  $P = 0.002$ , Figure 2a). In contrast, there was no significant difference in long-axis diameter between metastatic and non-metastatic lymph nodes ( $P = 0.99$ , Figure 2b). The ADC mean value was significantly lower in metastatic lymph nodes ( $1.26 \pm 0.20 \times 10^{-3}$  mm<sup>2</sup>/s) compared to non-metastatic lymph nodes ( $1.51 \pm 0.23 \times 10^{-3}$  mm<sup>2</sup>/s,  $P < 0.001$ , Figure 2c). Moreover, the ADC minimum value was significantly lower in metastatic lymph nodes ( $1.01 \pm 0.16 \times 10^{-3}$  mm<sup>2</sup>/s) compared to non-metastatic lymph nodes ( $1.33 \pm 0.23 \times 10^{-3}$  mm<sup>2</sup>/s,  $P < 0.001$ , Figure 2d).

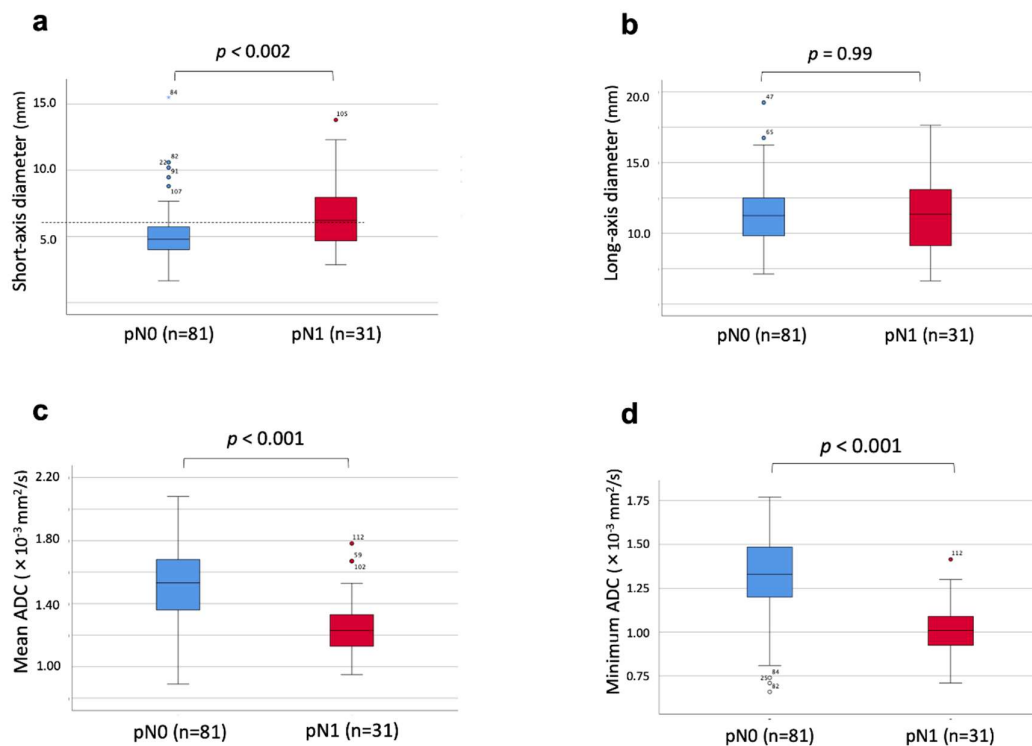


**Figure 2.** Correlation between lymph node diameters, ADC values, and histological lymph node metastasis. (a) The short-axis diameter was significantly larger in the lymph node metastasis group. (b) The long-axis diameter did not correlate with the presence of lymph node metastasis. (c) The ADC mean value was significantly lower in the lymph node metastasis group. (d) The ADC minimum value was significantly lower in the lymph node metastasis group.

The areas under the curve for the short-axis diameter, long-axis diameter, ADC mean, and ADC minimum were 0.69, 0.50, 0.80, and 0.88, respectively (Figure 3).

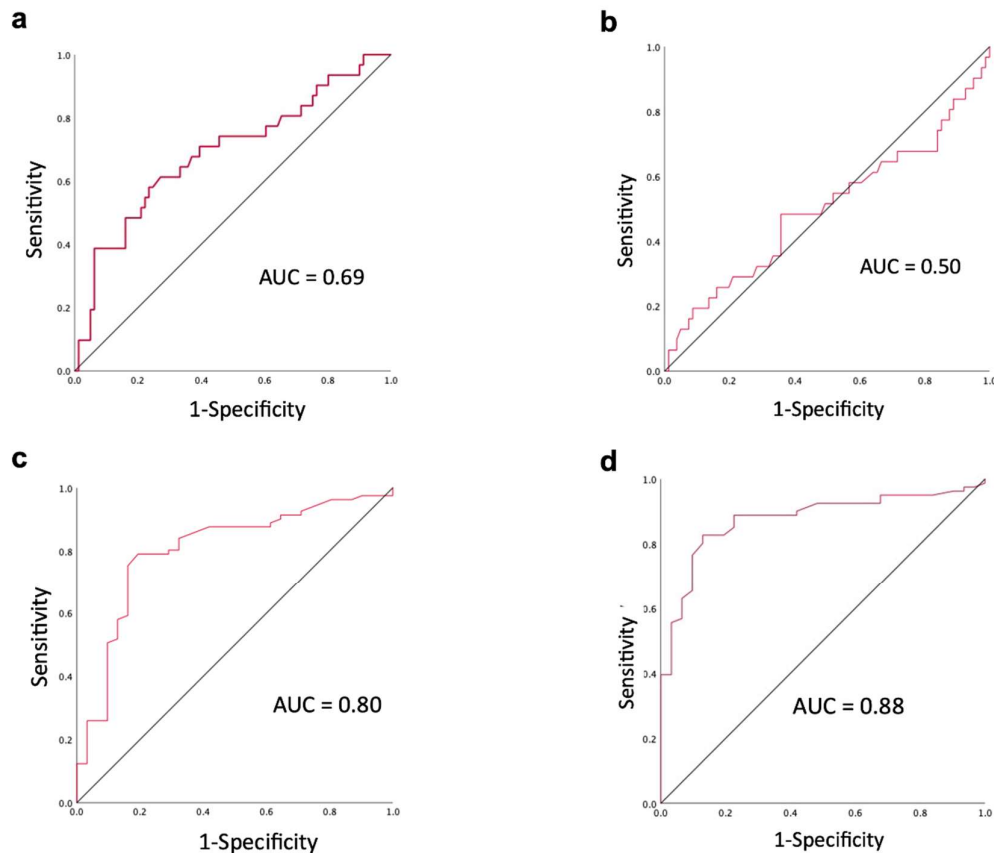


**Figure 3.** ROC curve for each diagnostic criterion. ROC curves for the short-axis diameter (a), long-axis diameter (b), ADC mean value (c), and ADC minimum value (d).

The cutoff values calculated from the ROC curves were as follows; the short-axis diameter: 5.8 mm, the ADC mean value:  $1.345 \times 10^{-3} \text{ mm}^2/\text{s}$ , and the ADC minimum value:  $1.140 \times 10^{-3} \text{ mm}^2/\text{s}$ . Using these cutoff values, the sensitivity, specificity, and accuracy for differentiating histological lymph node metastasis were 58.1%, 75.3%, and 70.5% for short-axis diameter, 80.6%, 79.0%, and 79.5% for the ADC mean, and 87.1%, 82.7%, and 83.9% for the ADC minimum, respectively (Table 3).

**Table 3.** Comparison of diagnostic performance.

| Diagnostic criteria for lymph node metastasis             | Sensitivity | Specificity | Accuracy |
|---|-------------|-------------|----------|
| Short-axis diameter > 5.785 mm                            | 58.1%       | 75.3%       | 70.5%    |
| Mean ADC < $1.345 \times 10^{-3} \text{ mm}^2/\text{s}$   | 80.6%       | 79.0%       | 79.5%    |
| Minimum ADC < $1.14 \times 10^{-3} \text{ mm}^2/\text{s}$ | 87.1%       | 82.7%       | 83.9%    |

ADC, apparent diffusion coefficient.

## Discussion

The present study demonstrated that the ADC minimum value within lymph nodes on DW-MRI had the highest accuracy in diagnosing preoperative lymph node metastasis in biliary tract cancer.

The formation of lymph node metastasis is involved in tumor-associated lymphangiogenesis [23–25]. It has been suggested that lymphangiogenesis occurs even before the formation of lymph node metastasis, making a pre-metastatic niche. Tumor cells undergo epithelial-mesenchymal transition, increasing their motility and invasiveness, thereby promoting invasion into the lymphatic vessels [26,27]. Tumor cells first metastasize to the draining lymph node (sentinel lymph node). Moreover, once tumor cells metastasize to the lymph nodes, lymphangiogenesis is further promoted [28]. It has been reported that large lymph node metastases can obstruct lymphatic drainage vessels, increasing intranodal pressure, thus lymphatic flow bypasses from the sentinel lymph node to other lymph nodes [29]. Additionally, a route for metastasis from lymph nodes to other organs has also been reported [30]. In head and neck cancers, a correlation has been observed between intratumoral lymphatic vessel density and lymph node metastasis [31]. Furthermore, overexpression of vascular endothelial growth factor (VEGF)-A, VEGF-C, or VEGF-D has been shown to promote the growth of tumor-associated lymphatic vessels and to facilitate lymph node metastasis [32]. The correlation between the expression of VEGF-C or VEGF-D and lymph node metastasis has also been demonstrated in colorectal cancer, gastric cancer, esophageal cancer, as well as in breast cancer, lung cancer, and uterine cancer [33].

Previous reports on the diagnosis of lymph node metastasis in biliary tract cancer using DW-MRI include the following: In 2016, the ADC mean value was reported to be useful for diagnosing lymph node metastasis in cholangiocarcinoma [33]. Additionally, recent studies have shown that the ADC mean value is diagnostically useful for lymph node metastasis in pancreato-biliary cancer and perihilar cholangiocarcinoma [34–36]. In contrast, Promsorn et al. reported that the ADC mean value did not contribute to the diagnosis of lymph node metastasis in cholangiocarcinoma [17]. They found that the mean ADC value is not very useful in distinguishing metastatic from nonmetastatic lymph nodes when the cancerous lesion is confined to a small portion of the lymph node. Theoretically, when the viable cancerous lesion within the metastatic lymph node occupies only a small portion of the lymph node, the ADC mean value of the lymph node is estimated to be lower, but the minimum ADC value remains unchanged. Therefore, the ADC minimum value can more accurately reflect the presence of lymph node metastasis, even if it is a small portion of the lymph node (Figure 1c, d). This may explain why the ADC minimum was even more diagnostically accurate than the ADC mean in the present study. Furthermore, abdominal CT is considered less likely to detect such micrometastases within lymph nodes compared to MRI because the lymph nodes with micrometastasis may not be enlarged.

PET has been reported to be more effective than CT in identifying lymph node metastasis in biliary tract cancer [37]. Regarding the comparison between PET and DW-MRI for diagnosing lymph node metastasis, DW-MRI was associated with higher sensitivity than PET in esophageal cancer [38]. On the other hand, combining MRI and PET information with CT can improve the diagnostic accuracy of lymph node metastasis [39]. Recent reports have demonstrated that CT radiomics achieved high diagnostic accuracy for lymph node metastasis in perihilar cholangiocarcinoma and intrahepatic cholangiocarcinoma [40,41]. Furthermore, the integration of artificial intelligence with radiomics has further enhanced diagnostic accuracy [42–45]. In rectal cancer, a model predicting lymph node metastasis by using machine learning software to perform deep learning on clinicopathological factors such as age, sex, tumor markers, T-factor, and short-axis diameter of lymph nodes using, was proven to be more useful than conventional diagnostic criteria [46]. In addition, the efficacy of MRI radiomics in diagnosing lymph node metastasis has been reported in pancreatic cancer and rectal cancer [47,48].

Incorporating these advanced technologies with DW-MRI is expected to lead to more accurate preoperative diagnosis of lymph node metastasis in biliary tract cancer.

This study has several limitations. First, this study is a retrospective study with a limited sample size. To derive generalizable results, larger prospective studies involving more extensive cohorts are

needed in the future. Secondly, the study uses specific MRI equipment and protocols, which means that further verification is required to assess reproducibility across different MRI devices. Furthermore, the pathological diagnosis of lymph node metastasis using HE staining may miss micrometastases. Yamamoto H reported that when a one-step nucleic acid amplification assay was performed on colorectal cancer cases, the rates of upstaging for pathological Stage I, IIA, IIB, and IIC were 2.0%, 17.7%, 12.5%, and 25%, respectively [49]. However, the minimum ADC value may have the potential to detect such micrometastases accurately, and further studies should be conducted to evaluate diagnostic capability of the minimum ADC value for lymph node micrometastases.

In conclusion, the present study demonstrated that the short-axis diameter, ADC mean value, and ADC minimum value of lymph nodes were significantly different between histologically metastatic and non-metastatic lymph nodes. However, the ADC minimum value showed the best discriminative ability, with the highest sensitivity, specificity, and accuracy. These findings suggest that the ADC minimum value is highly effective for differentiating metastatic lymph nodes in biliary tract cancer.

**Author Contributions** Conceptualization, T.M. and H.S.; Methodology, K.S.; Software, T.M.; Validation, H.N. and K.S.; Formal Analysis, T.M. and H.N.; Investigation, T.M.; Data Curation, T.M.; Writing – Original Draft Preparation, T.M.; Writing – Review & Editing, H.S.; Visualization, T.M and A.U.; Supervision, H.S. and K.K.; Project Administration, H.S. and C.K.

**Funding:** The authors did not receive support from any organization for the submitted work.

**Institutional Review Board Statement:** The study was conducted according to the guidelines of the Declaration of Helsinki, and approved by the Institutional Review Board.

**Informed Consent Statement:** Not applicable.

**Data Availability Statement:** The datasets generated and/or analyzed during the current study are available from the corresponding author on reasonable request.

**Conflicts of Interest:** The authors declare no conflict of interest.

## List of Abbreviations

CT, computed tomography; MRI, magnetic resonance imaging; ERCP, endoscopic retrograde cholangiopancreatography; PET, positron emission tomography; DW-MRI, diffusion-weighted magnetic resonance imaging; ADC, apparent diffusion coefficient; TE, echo time; TR, repetition time; ROI, region of interest; ROC, receiver operating characteristic, VEGF, vascular endothelial growth factor.

## References

1. Lamarca A, Edeline J, Goyal L. How I treat biliary tract cancer. *ESMO Open*. (2022) 7:100378. doi: 10.1016/j.esmoop.2021.100378.
2. Yokoyama Y, Nishio H, Ebata T, Igami T, Sugawara G, Nagino M. Value of indocyanine green clearance of the future liver remnant in predicting outcome after resection for biliary cancer. *Br J Surg*. (2010) 97:1260-8. doi: 10.1002/bjs.7084.
3. Kato A, Shimizu H, Ohtsuka M, Yoshitomi H, Furukawa K, Takayashiki T, et al. Downsizing Chemotherapy for Initially Unresectable Locally Advanced Biliary Tract Cancer Patients Treated with Gemcitabine Plus Cisplatin Combination Therapy Followed by Radical Surgery. *Ann Surg Oncol*. (2015) Suppl 3:S1093-9. doi: 10.1245/s10434-015-4768
4. Ishihara S, Horiguchi A, Miyakawa S, Endo I, Miyazaki M, Takada T. Biliary tract cancer registry in Japan from 2008 to 2013. *J Hepatobiliary Pancreat Sci*. (2016) 23:149-57. doi: 10.1002/jhbp.314.
5. Nagino M, Ebata T, Yokoyama Y, Igami T, Sugawara G, Takahashi Y, et al. Evolution of surgical treatment for perihilar cholangiocarcinoma: a single-center 34-year review of 574 consecutive resections. *Ann Surg*. (2013) 258:129-40. doi: 10.1097/SLA.0b013e3182708b57.
6. Endo I, Shimada H, Tanabe M, Fujii Y, Takeda K, Morioka D, et al. Prognostic significance of the number of positive lymph nodes in gallbladder cancer. *J Gastrointest Surg*. (2006) 10:999-1007. doi: 10.1016/j.gassur.2006.03.006.
7. Sierzega M, Nowak K, Kulig J, Matyja A, Nowak W, Popiela T. Lymph node involvement in ampullary cancer: the importance of the number, ratio, and location of metastatic nodes. *J Surg Oncol*. (2009) 100:19-24. doi: 10.1002/jso.21283.

8. Ganeshalingam S, Koh DM. Nodal staging. *Cancer Imaging*. 2009 Dec 24;9(1):104-11. doi: 10.1102/1470-7330.2009.0017.
9. Murakami Y, Uemura K, Hayashidani Y, Sudo T, Ohge H, Sueda T. Pancreatoduodenectomy for distal cholangiocarcinoma: prognostic impact of lymph node metastasis. *World J Surg*. (2007)31:337-42; discussion 343-4. doi: 10.1007/s00268-006-0224-0.
10. Sierzega M, Nowak K, Kulig J, Matyja A, Nowak W, Popiela T. Lymph node involvement in ampullary cancer: the importance of the number, ratio, and location of metastatic nodes. *J Surg Oncol*. (2009) 100:19-24. doi: 10.1002/jso.21283.
11. Matsuyama R, Morioka D, Mori R, Yabushita Y, Hiratani S, Ota Y, et al. Our Rationale of Initiating Neoadjuvant Chemotherapy for Hilar Cholangiocarcinoma: A Proposal of Criteria for "Borderline Resectable" in the Field of Surgery for Hilar Cholangiocarcinoma. *World J Surg*. (2019) 43:1094-1104. doi: 10.1007/s00268-018-04883-y.
12. Matsuyama R, Mori R, Ota Y, Homma Y, Yabusita Y, Hiratani S, et al. Impact of Gemcitabine Plus S1 Neoadjuvant Chemotherapy on Borderline Resectable Perihilar Cholangiocarcinoma. *Ann Surg Oncol*. (2022) 29:2393-2405. doi: 10.1245/s10434-021-11206-4.
13. Morimoto H, Ajiki T, Ueda T, Sawa H, Fujita T, Matsumoto I, et al. Histological features of lymph node metastasis in patients with biliary tract cancer. *J Surg Oncol*. (2008) 97:423-7. doi: 10.1002/jso.20963.
14. Sugai K, Sekine Y, Kawamura T, Yanagihara T, Saeki Y, Kitazawa S, et al. Sphericity of lymph nodes using 3D-CT predicts metastasis in lung cancer patients. *Cancer Imaging*. (2023) 23:124. doi: 10.1186/s40644-023-00635-x.
15. Ganeshalingam S, Koh DM. Nodal staging. *Cancer Imaging*. (2009) 9:104-11. doi: 10.1102/1470-7330.2009.0017.
16. Noji T, Kondo S, Hirano S, Tanaka E, Suzuki O, Shichinohe T. Computed tomography evaluation of regional lymph node metastases in patients with biliary cancer. *Br J Surg*. (2008) 95:92-6. doi: 10.1002/bjs.5920.
17. Promsorn J, Soontrapa W, Somsap K, Chamadol N, Limpawattana P, Harisinghani M. Evaluation of the diagnostic performance of apparent diffusion coefficient (ADC) values on diffusion-weighted magnetic resonance imaging (DWI) in differentiating between benign and metastatic lymph nodes in cases of cholangiocarcinoma. *Abdom Radiol* (2019) 44:473-481. doi: 10.1007/s00261-018-1742-6.
18. Kurosawa J, Tawada K, Mikata R, Ishihara T, Tsuyuguchi T, Saito M, et al. Prognostic relevance of apparent diffusion coefficient obtained by diffusion-weighted MRI in pancreatic cancer. *J Magn Reson Imaging*. (2015) 42:1532-7. doi: 10.1002/jmri.24939.
19. Kim SJ, Lee JM, Kim H, Yoon JH, Han JK, Choi BI. Role of diffusion-weighted magnetic resonance imaging in the diagnosis of gallbladder cancer. *J Magn Reson Imaging*. (2013) 38:127-37. doi: 10.1002/jmri.23956.
20. Yu MH, Kim YJ, Park HS, Jung SI. Benign gallbladder diseases: Imaging techniques and tips for differentiating with malignant gallbladder diseases. *World J Gastroenterol*. (2020) 26:2967-2986. doi: 10.3748/wjg.v26.i22.2967.
21. Yoo RE, Lee JM, Yoon JH, Kim JH, Han JK, Choi BI. Differential diagnosis of benign and malignant distal biliary strictures: value of adding diffusion-weighted imaging to conventional magnetic resonance cholangiopancreatography. *J Magn Reson Imaging*. (2014) 39:1509-17. doi: 10.1002/jmri.24304.
22. Miyazaki K, Morine Y, Yamada S, Saito Y, Tokuda K, Okikawa S, et al. Stromal tumor-infiltrating lymphocytes level as a prognostic factor for resected intrahepatic cholangiocarcinoma and its prediction by apparent diffusion coefficient. *Int J Clin Oncol*. (2021) 26:2265-2274. doi: 10.1007/s10147-021-02026-3.
23. Holzapfel K, Gaa J, Schubert EC, Eiber M, Kleeff J, Rummeny EJ, et al. Value of diffusion-weighted MR imaging in the diagnosis of lymph node metastases in patients with cholangiocarcinoma. *Abdom Radiol*. (2016) 41:1937-41. doi: 10.1007/s00261-016-0791-y.
24. Lee JH, Han SS, Hong EK, Cho HJ, Joo J, Park EY, et al. Predicting lymph node metastasis in pancreatobiliary cancer with magnetic resonance imaging: A prospective analysis. *Eur J Radiol*. (2019) 116:1-7. doi: 10.1016/j.ejrad.2019.04.007.
25. Mandriota SJ, Jussila L, Jeltsch M, Compagni A, Baetens D, Prevo R, et al. Vascular endothelial growth factor-C-mediated lymphangiogenesis promotes tumour metastasis. *EMBO J*. (2001) 20:672-82. doi: 10.1093/emboj/20.4.672.
26. Skobe M, Hawighorst T, Jackson DG, Prevo R, Janes L, Velasco P, et al. M. Induction of tumor lymphangiogenesis by VEGF-C promotes breast cancer metastasis. *Nat Med*. (2001)7:192-8. doi: 10.1038/84643.
27. Stacker SA, Caesar C, Baldwin ME, Thornton GE, Williams RA, Prevo R, et al. VEGF-D promotes the metastatic spread of tumor cells via the lymphatics. *Nat Med*. (2001) 7:186-91. doi: 10.1038/84635.
28. Pastushenko I, Blanpain C. EMT Transition States during Tumor Progression and Metastasis. *Trends Cell Biol*. (2019) 29:212-226. doi: 10.1016/j.tcb.2018.12.001.
29. Tsai JH, Yang J. Epithelial-mesenchymal plasticity in carcinoma metastasis. *Genes Dev*. (2013) 27:2192-206. doi: 10.1101/gad.225334.113.

30. Karaman S, Detmar M. Mechanisms of lymphatic metastasis. *J Clin Invest.* (2014) 124:922-8. doi: 10.1172/JCI71606.
31. Nathanson SD, Mahan M. Sentinel lymph node pressure in breast cancer. *Ann Surg Oncol.* (2011) 18:3791-6. doi: 10.1245/s10434-011-1796-y.
32. Jones D, Pereira ER, Padera TP. Growth and Immune Evasion of Lymph Node Metastasis. *Front Oncol.* (2018) 8:36. doi: 10.3389/fonc.2018.00036.
33. Beasley NJ, Prevo R, Banerji S, Leek RD, Moore J, van Trappen P, et al. Intratumoral lymphangiogenesis and lymph node metastasis in head and neck cancer. *Cancer Res.* (2002) 62:1315-20.
34. Zhou H, Lei PJ, Padera TP. Progression of Metastasis through Lymphatic System. *Cells.* (2021) 10:627. doi: 10.3390/cells10030627.
35. Hosokawa I, Hayano K, Furukawa K, Takayashiki T, Kuboki S, Takano S, et al. Preoperative Diagnosis of Lymph Node Metastasis of Perihilar Cholangiocarcinoma Using Diffusion-Weighted Magnetic Resonance Imaging. *Ann Surg Oncol.* (2022) 29:5502-5510. doi: 10.1245/s10434-022-11931-4.
36. Morine Y, Shimada M, Imura S, Ikemoto T, Hanaoka J, Kanamoto M, Ishibashi H, Utsunomiya T. Detection of Lymph Nodes Metastasis in Biliary Carcinomas: Morphological Criteria by MDCT and the Clinical Impact of DWI-MRI. *Hepatogastroenterology.* 2015 Jun;62(140):777-81.
37. Kobayashi S, Nagano H, Hoshino H, Wada H, Marubashi S, Eguchi H, Takeda Y, Tanemura M, Kim T, Shimosegawa E, Hatazawa J, Doki Y, Mori M. Diagnostic value of FDG-PET for lymph node metastasis and outcome of surgery for biliary cancer. *J Surg Oncol.* 2011 Mar 1;103(3):223-9. doi: 10.1002/jso.21811.
38. Shuto K, Kono T, Shiratori T, Akutsu Y, Uesato M, Mori M, et al. Diagnostic performance of diffusion-weighted magnetic resonance imaging in assessing lymph node metastasis of esophageal cancer compared with PET. *Esophagus.* (2020) 17:239-249. doi: 10.1007/s10388-019-00704-w.
39. Yoo J, Lee JM, Yoon JH, Joo I, Lee DH. Additional Value of Integrated 18F-FDG PET/MRI for Evaluating Biliary Tract Cancer: Comparison with Contrast-Enhanced CT. *Korean J Radiol.* (2021) 22:714-724. doi: 10.3348/kjr.2020.0689.
40. Zhan PC, Yang T, Zhang Y, Liu KY, Li Z, Zhang YY, et al. Radiomics using CT images for preoperative prediction of lymph node metastasis in perihilar cholangiocarcinoma: a multi-centric study. *Eur Radiol.* (2024) 34:1280-1291. doi: 10.1007/s00330-023-10108-1.
41. Ji GW, Zhu FP, Zhang YD, Liu XS, Wu FY, Wang K, et al. A radiomics approach to predict lymph node metastasis and clinical outcome of intrahepatic cholangiocarcinoma. *Eur Radiol.* (2019) 29:3725-3735. doi: 10.1007/s00330-019-06142-7.
42. Bian Y, Zheng Z, Fang X, Jiang H, Zhu M, Yu J, et al. Artificial Intelligence to Predict Lymph Node Metastasis at CT in Pancreatic Ductal Adenocarcinoma. *Radiology.* (2023) 306:160-169. doi: 10.1148/radiol.220329.
43. Bedrikovetski S, Dudi-Venkata NN, Kroon HM, Seow W, Vather R, Carneiro G, et al. Artificial intelligence for pre-operative lymph node staging in colorectal cancer: a systematic review and meta-analysis. *BMC Cancer.* (2021) 21:1058. doi: 10.1186/s12885-021-08773-w.
44. Wang C, Yu P, Zhang H, Han X, Song Z, Zheng G, Wang G, Zheng H, Mao N, Song X. Artificial intelligence-based prediction of cervical lymph node metastasis in papillary thyroid cancer with CT. *Eur Radiol.* 2023 Oct;33(10):6828-6840. doi: 10.1007/s00330-023-09700-2.
45. Chu LC, Fishman EK. Artificial Intelligence Outperforms Radiologists for Pancreatic Cancer Lymph Node Metastasis Prediction at CT. *Radiology.* 2023 Jan;306(1):170-171. doi: 10.1148/radiol.222012.
46. Kasai S, Shiomi A, Kagawa H, Hino H, Manabe S, Yamaoka Y, et al. The Effectiveness of Machine Learning in Predicting Lateral Lymph Node Metastasis From Lower Rectal Cancer: A Single Center Development and Validation Study. *Ann Gastroenterol Surg.* (2021) 6:92-100. doi: 10.1002/ags3.12504.
47. Shi L, Wang L, Wu C, Wei Y, Zhang Y, Chen J. Preoperative Prediction of Lymph Node Metastasis of Pancreatic Ductal Adenocarcinoma Based on a Radiomics Nomogram of Dual-Parametric MRI Imaging. *Front Oncol.* 2022 Jul 6;12:927077. doi: 10.3389/fonc.2022.927077.
48. Fang Z, Pu H, Chen XL, Yuan Y, Zhang F, Li H. MRI radiomics signature to predict lymph node metastasis after neoadjuvant chemoradiation therapy in locally advanced rectal cancer. *Abdom Radiol.* (2023) 48:2270-2283. doi: 10.1007/s00261-023-03910-4.
49. Yamamoto H. Micrometastasis in lymph nodes of colorectal cancer. *Ann Gastroenterol Surg.* (2022) 6:466-473. doi: 10.1002/ags3.12576.

**Disclaimer/Publisher's Note:** The statements, opinions and data contained in all publications are solely those of the individual author(s) and contributor(s) and not of MDPI and/or the editor(s). MDPI and/or the editor(s) disclaim responsibility for any injury to people or property resulting from any ideas, methods, instructions or products referred to in the content.